

# Optimization of the Method of Auxiliary Sources for 3D Scattering Problems by Using Generalized Impedance Boundary Conditions and Level Set Technique

Afif Bouzidi\* and Taoufik Aguil

**Abstract**—The method of auxiliary sources (MAS) presents a promising alternative to methods based on discretization, currently used for solving scattering problems. The optimal choice of the auxiliary surface and the proper allocation of radiation centers play a crucial role in ensuring accuracy and stability of the MAS. This approach is considered an open issue and can be investigated numerically. In this paper, we propose a systematic and fully automated technique leading to determine the optimal parameters of the MAS for arbitrary shaped obstacles (partially or fully penetrable) for scattering problems.

## 1. INTRODUCTION

Solving scattering problems with an optimal compromise between accuracy and computational resources has been a requirement of many engineering fields such as inverse problems, microwave imaging, Radar cross section computing and EMC. Numerical techniques based on rigorous formulation like the method of moments (MOM), TLM or FDTD provide accurate results, however in many cases, the computational cost is assessed as prohibitive. The mesh-free methods like the method of auxiliary sources state an auspicious alternative to these techniques. The MAS is a numerical method which was originally developed by a Georgian research group for solving scattering and radiation electromagnetic problems [1–3]. The fundamental idea of the MAS is the interchange of boundary conditions and differential equation, which excludes the singularities of the integral equation by shifting the auxiliary sources contour relative to integration one [4]. The scattered field is expanded in terms of the fundamental solutions of Helmholtz-equation [5]. The boundary value problem is solved by imposing the boundary condition at the scattering surface in the same manner as the standard surface integral methods. Previous researches [6–8] have shown that the appropriate choice of the auxiliary surface and the location of radiation centers is decisive to achieve efficiency of the MAS. The optimal choice of the MAS parameters (auxiliary surface, radiation centers) remains an open issue probed by several scientific manuscripts [9–11, 20, 25]. The distribution of the auxiliary sources strongly affects the accuracy and the convergence of the numerical solution, it is shown that to ensure the MAS efficiency, the auxiliary surface should enclose the scattered field singularities as tightly as possible [12, 13, 26]. The standard placement of the auxiliary sources is based on empirical conventions and on the caustic hypothesis. As a result, the optimal distribution of the auxiliary sources, for a predefined accuracy is achieved by try-and-error processes or by determining the corresponding caustic surfaces [8, 21–24]. These approaches are analytically feasible only when treating problems with canonical geometries (sphere, ellipsoid or infinite plan . . .). The localization of scattered field singularities for arbitrary-shaped objects is the prevailing breakdown point of the MAS. The salient feature of the proposed technique is the replacement of

---

*Received 22 September 2014, Accepted 29 October 2014, Scheduled 5 November 2014*

\* Corresponding author: Afif Bouzidi (afif.bouzidi@gmail.com).

The authors are with the Syscom Laboratory, National Engineering School of Tunis (ENIT), Tunis El Manar University, B. P. 37, Le Belvedere, Tunis 1002, Tunisia.

laborious trial and error stage of the standard MAS by a systematic optimization procedure. The outline of the paper is as follows. First we go over scattering problems with impedance boundary conditions and we present the formulation of the MAS also we discuss the impact of the singularities localization on the efficiency of the MAS. Secondly we review the level set method and we adapt it to our problem. After that we set up a framework to find optimum MAS parameters by combining surface impedance boundary conditions and level set technique. Finally, we report some numerical experiments to clearly demonstrate the accuracy and the robustness of the optimized MAS compared to the standard one.

## 2. AUXILIARY SOURCES METHOD FORMULATION

Let consider  $\Omega$  an open subset of  $\mathbb{R}^3$ , occupied by a medium with the permittivity  $\varepsilon$ , permeability  $\mu$  and conductivity  $\sigma$ .  $\Omega$  represents the obstacle, and a Generalized Impedance Boundary Condition is held on its surface  $\Gamma$ .  $\Omega$  is illuminated by a linearly polarized electromagnetic plane wave  $\vec{E}_i = \vec{E}_0 e^{-j\vec{k}\cdot\vec{r}}$ . The propagation constant, permittivity, permeability and intrinsic impedance of the surrounding medium are  $k$ ,  $\varepsilon_0$ ,  $\mu_0$  and  $Z_0$  respectively. A time factor  $e^{-j\omega t}$  has been assumed and suppressed.

$\vec{E}$  denotes the total field, sum of incident and scattered field. The governing equations for  $\vec{E}$  are

$$\begin{cases} \nabla \times \vec{E} + j\omega\mu_0\vec{H} = 0 & r \in \mathbb{R}^3 \setminus \Omega \\ \nabla \times \vec{H} - j\omega\varepsilon_0\vec{E} = 0 & r \in \mathbb{R}^3 \setminus \Omega \\ (\vec{n} \times \vec{E}) \times \vec{n} = Z^{\delta,m} (\vec{n} \times \vec{H}) & r \in \Gamma \end{cases} \quad (1)$$

where  $\vec{n}$  denotes the unit normal to  $\Gamma$  oriented to the exterior of  $\Omega$ .

$Z^{\delta,m}$  is the local impedance operator of order  $m$  that relates the tangential traces of the electric and magnetic fields. The order  $m$  increases with the desired order of accuracy. The surface impedance was presented to model objects with strong skin depth. The main idea behind this concept is replacing the obstacles volume by an effective boundary condition applied to the interface obstacle/dielectric. Therefore, the interior field distribution can be omitted. We will focus only on exterior field. Rytov has developed a general method to construct low and high order surface impedance boundary conditions (SIBC) [14]. By using perturbation techniques, He revealed that the SIBC is an asymptotic expansion in terms of the skin depth  $\delta$ . Recently, Antoine-Barucq-Vernhet [15] proposed a new derivation of SIBC based on the pseudo-differential operators leading to the Generalized Impedance Boundary Conditions (GIBCs) that can be used to model partially or totally penetrable obstacles.

The zero order expansion represents perfect electric conductors, where no electromagnetic field could penetrate

$$Z^{\delta,0} = 0 \quad (2)$$

The first expansion order represents Leontovich impedance, where the electromagnetic field variation parallel to the surface is assumed to be small compared to the variation perpendicular to the surface [15]

$$Z^{\delta,1} = \left( \frac{\sqrt{2}}{2} - j\frac{\sqrt{2}}{2} \right) \delta \quad (3)$$

The second expansion order is Mitzner impedance, take into consideration the radii of curvature [15]

$$Z^{\delta,2} = Z^{\delta,1} + j\delta^2(C - H) \quad (4)$$

where  $C$  is the curvature tensor and  $H = hI_\Gamma$ .  $h$  is the mean curvature of  $\Gamma$ ,  $I_\Gamma$  is the projection operator on the tangent plane to  $\Gamma$ . The third expansion order is Rytov impedance, take into consideration the variations of electromagnetic fields on the surface [15]

$$Z^{\delta,3} = Z^{\delta,2} - \left( \frac{\sqrt{2}}{4} + j\frac{\sqrt{2}}{4} \right) \delta^3 \left[ C^2 - H^2 + (\varepsilon\mu)\omega^2 + \nabla_\Gamma \operatorname{div}_\Gamma + \overrightarrow{\operatorname{curl}}_\Gamma \operatorname{curl}_\Gamma \right] \quad (5)$$

We denote respectively by  $\nabla_\Gamma$  and  $\operatorname{div}_\Gamma$  the surface gradient and the surface divergence on  $\Gamma$ . We then define the surface curl of a tangential vector  $\vec{V}$  and the surface vector curl of a scalar function  $u$  defined

on  $\Gamma$  by

$$\overrightarrow{\text{curl}}_{\Gamma} u = (\nabla_{\Gamma} u) \times \vec{n} \tag{6}$$

$$\text{curl}_{\Gamma} \vec{V} = \text{div}_{\Gamma} (\vec{V} \times \vec{n}) \tag{7}$$

Given the linearity of  $Z^{\delta,m}$ , the last equation in (1) can be written in the following form

$$\mathfrak{L}(\vec{E}^s) = \vec{f}(r), \quad \forall r \in \Gamma \tag{8}$$

where

$$\mathfrak{L}(\vec{E}^s) = \vec{n} \times (\vec{n} \times \vec{E}^s) + \frac{j}{\omega\mu_0} Z^{\delta,m} (\vec{n} \times (\nabla \times \vec{E}^s)) \tag{9}$$

and

$$\vec{f}(r) = -\vec{n} \times (\vec{n} \times \vec{E}^i) - \frac{j}{\omega\mu_0} Z^{\delta,m} (\vec{n} \times (\nabla \times \vec{E}^i)) \tag{10}$$

According to the auxiliary sources method, let  $S$  designate the auxiliary surface,  $M_{1 \leq i \leq n}$  the radiation centers located at points  $r_{1 \leq i \leq n}$  as shown in Figure 1 and  $\vec{U}(|\vec{r}_i - \vec{r}|)_{1 \leq i \leq n}$  the Helmholtz equation solution associated with elementary sources.

$$\vec{U}(|\vec{r}_i - \vec{r}|) = \frac{e^{-jk|\vec{r}_i - \vec{r}|}}{4\pi|\vec{r}_i - \vec{r}|} (\vec{r}_i - \vec{r}) \tag{11}$$

Kupradze [5] proved that the set of functions  $\vec{U}(|\vec{r}_i - \vec{r}|)_{1 \leq i \leq \infty}$  is complete and linearly independent on the surface  $\Gamma$ . So, there are Coefficients  $a_{1 \leq i \leq n}$  such that, using the  $n$  first functions of the aforementioned system, the scattered electric field can be approximated as follows.

$$\vec{E}^s \approx \sum_{i=1}^n a_i \vec{U}(|\vec{r}_i - \vec{r}|) \tag{12}$$

which will approach exact solution as  $n \rightarrow \infty$ .

The scattered field satisfies the Sommerfeld radiation condition

$$\lim_{r \rightarrow \infty} \left( \sqrt{\frac{\mu_0}{\epsilon_0}} \vec{H}^s \times \frac{\vec{r}}{r} - \vec{E}^s \right) = 0 \tag{13}$$

It has been proved that any scattered field that transfers energy to infinity must have areas of irregular sources within finite volume, otherwise the scattered field is null everywhere [16]. So, it is obvious that  $\vec{E}^s$  certainly has irregular domains that could be in form of isolated points, lines or surfaces.  $S$  should enclose the singularities as tightly as possible. Ignoring this point leads to a weakening of convergence and even diverging of the Equation (12) when  $n$  increases. The expansion Coefficients  $a_{1 \leq i \leq n}$  are calculated by imposing the boundary condition at  $\Gamma$ . Let  $\vec{G}(|\vec{r}_i - \vec{r}|)$  defined by

$$\vec{G}(|\vec{r}_i - \vec{r}|) = \mathfrak{L}(\vec{U}(|\vec{r}_i - \vec{r}|)) \tag{14}$$

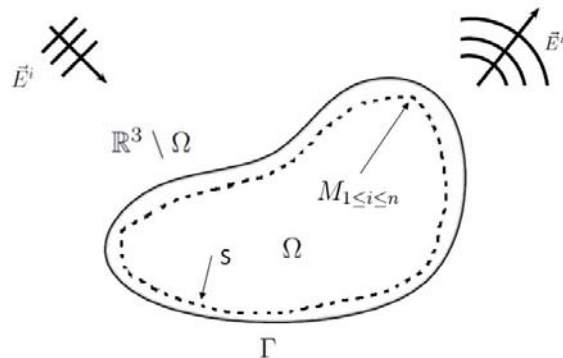


Figure 1. MAS geometry.

The boundary conditions (8) can be written as:

$$\sum_{i=1}^n a_i \vec{G}(|\vec{r}_i - \vec{r}|) = \vec{f}(r), \quad \forall r \in \Gamma \quad (15)$$

By matching the boundary condition at  $m$  collocation points  $r_{1 \leq p \leq m}$  the problem can be formulated as follows: Find  $a_{1 \leq i \leq n}$  such that

$$\sum_{i=1}^n a_i \vec{G}(|\vec{r}_i - \vec{r}_p|) = \vec{f}(r_p), \quad 1 \leq p \leq m \quad (16)$$

The stability and size of the obtained algebraic system depend on the proper choice of auxiliary parameters that are the shape of the auxiliary surface  $S$  and the distribution of the radiation centers  $r_{1 \leq i \leq n}$ . The necessary number of terms of the series (12) strongly depends on the relative distance between the real surface and the auxiliary surface  $S$  on which the auxiliary sources are placed. When the auxiliary surface moves away from the real one the number of terms in (12) decreases strongly and consequently, the computational cost decreases but it should be noted that if the scattered field singularities appear outside the auxiliary surface, the computing process might diverge. Therefore a good description of singularities is an essential part of the method to carry out the optimal solution.

### 3. THE LEVEL SET METHOD

#### 3.1. An Overview of Level Set Method

The level set method was introduced by Osher and Sethian [16] in the field of fluid dynamics, to trace interfaces between different phases of fluid flows. Later, it has been used for many different kinds of physical problems, see [17–19]. The main idea behind this method is to represent the interface at each time  $t$  as the zero level set of a function  $\varphi$ . Thus, given a surface  $S$  in  $\mathbb{R}^3$  bounding an open region  $D \subset \Omega$ , we wish to study its motion under a velocity field  $v$ . The level set idea consists in defining a smooth function  $\varphi(r, t) : \mathbb{R}^3 \times \mathbb{R}^+ \rightarrow \mathbb{R}$  to implicitly represent the interface  $S$  as the set of points  $r \in \mathbb{R}^3$  where  $\varphi(r, t)$  vanishes. That is  $S = \{r \in \mathbb{R}^3 / \varphi(r, t) = 0\}$ . The function  $\varphi$  is called the level set function, and it has the following properties

$$\begin{aligned} \varphi < 0 & \quad \text{for } x \in D \\ \varphi > 0 & \quad \text{for } x \notin D \\ \varphi = 0 & \quad \text{for } x \in S \end{aligned} \quad (17)$$

This concept illustrated by Figure 2.

The evolution of the implicit function  $\varphi$  can be described by the following partial differential equation, known as Hamilton-Jacobi equation [17]

$$\frac{\partial \varphi}{\partial t} + \|\nabla \varphi\| v = 0, \quad \varphi(r, 0) = \varphi_0 \quad (18)$$

where,  $\frac{\partial}{\partial t}$  denotes a partial derivative to the temporal variable  $t$ , and  $\nabla$  denotes the gradient operator. The function  $\varphi_0$  embeds the initial position of the moving surface  $S$ .

#### 3.2. The Level Set Dictionary

Once the level set function  $\varphi$  is defined, most of the geometrical quantities of the surface  $S$  can be represented in terms of the function  $\varphi$  [17]

The normal vector is given by:

$$\vec{n} = \frac{\nabla \varphi}{\|\nabla \varphi\|} \quad (19)$$

The mean curvature:

$$\kappa = \nabla \cdot \vec{n} = \nabla \cdot \frac{\nabla \varphi}{\|\nabla \varphi\|} \quad (20)$$

The area of  $S$

$$L(\varphi) = \int_{\Omega} \delta(\varphi) \|\nabla\varphi\| dS \tag{21}$$

where  $\delta(\varphi)$  denotes the Dirac function

$$\delta(\varphi) = \begin{cases} 1 & \text{if } \varphi = 0 \\ 0 & \text{if } \varphi \neq 0 \end{cases} \tag{22}$$

Moreover the surface integral of a function  $f$  along  $S$  can be written in function of  $\varphi$

$$\int_S f(r) dS = \int_{\Omega} f(r) \delta(\varphi) \|\nabla\varphi\| dr \tag{23}$$

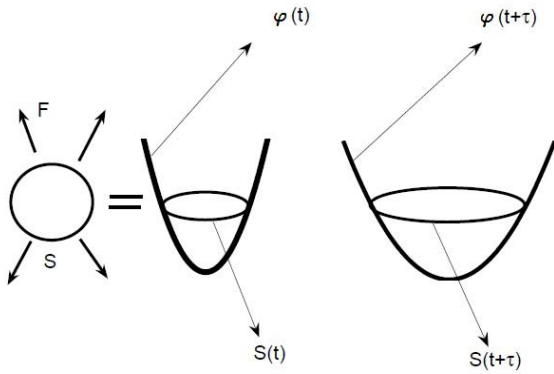


Figure 2. Level set function.

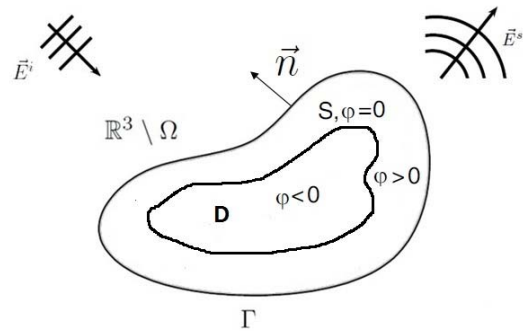


Figure 3. Level-set representation of the auxiliary surface.

#### 4. OPTIMIZATION METHOD

The algebraic system (16) can be written in the following form

$$\int_S A(r') \vec{G}(|r' - x_p|) dS = \vec{f}(x_p) \quad 1 \leq p \leq m \tag{24}$$

where

$$A(r') = \sum_{i=1}^n a_i \delta(r_i - r') \tag{25}$$

$$\delta(r_i - r') = \begin{cases} 1 & \text{if } r' = r_i \\ 0 & \text{if } r' \neq r_i \end{cases} \tag{26}$$

Let consider  $D$  an open subset of  $\Omega$  enclosed by the auxiliary surface  $S$  as shown in Figure 3.

We define  $\varphi$  as a level set function of  $S$  by

$$\varphi(r, t) = \begin{cases} -\text{distance}(r, S) & \text{if } r \in D \\ \text{distance}(r, S) & \text{if } r \notin D \end{cases} \tag{27}$$

$S$  divides the domain  $D$  into two parts, and then the level set function  $\varphi$  is negative inside and positive outside.

$$S = \{r \in \mathbb{R}^3, \quad \varphi(r, t) = 0\} \tag{28}$$

By using the property (23) of the level set method, the Equation (24) can be written as

$$\int_{\Omega} A(r') \vec{G}(|r' - x_p|) \delta(\varphi) \|\nabla\varphi\| dr' = \vec{f}(x_p) \quad 1 \leq p \leq m \tag{29}$$

The problem can be formulated as an optimization one

$$(a_{1 \leq k \leq n}^*, \varphi^*) = \arg \min_{a_k, \varphi} J(A, \varphi) \quad (30)$$

Find amplitudes  $a_{1 \leq k \leq n}^*$  and level set function  $\varphi^*$  that minimize the cost functional  $J$ .

$$J(A, \varphi) = \frac{1}{m} \sum_{p=1}^m \left\| \int_{\Omega} A(r') \vec{G}(|r' - x_p|) \delta(\varphi) \|\nabla \varphi\| dr' - \vec{f}(x_p) \right\|^2 \quad (31)$$

The optimal distribution of the radiation centers  $r_{1 \leq k \leq n}$  strongly depends on the area of the auxiliary surface. By shifting the sources into the conducting body the scattered field function becomes more smooth on the surface of the body and the fulfillment of the boundary conditions in the region between collocation points is improved. However, the shift of the auxiliary surface is restricted by the location of the scattered field singularities. So, the area of the auxiliary surface should be added to the cost functional  $J$  as regularisation term. Therefore, we force the algorithm to search the best-suited auxiliary surface that encloses the singularities.

$$J(A, \varphi) = \frac{1}{m} \sum_{p=1}^m \left\| \int_{\Omega} A(r') \vec{G}(|r' - x_p|) \delta(\varphi) \|\nabla \varphi\| dr' - \vec{f}(x_p) \right\|^2 + \beta L(\varphi) \quad (32)$$

where  $\beta$  is a real-valued regularization coefficient.

#### 4.1. Calculation of the Auxiliary Surface

The evolution of  $\varphi$  is described by the following Hamilton-Jacobi equation.

$$\frac{\partial \varphi}{\partial t} + \|\nabla \varphi\| v = 0, \quad \varphi(r, 0) = \varphi_0 \quad (33)$$

in this differential form  $t$  does not represent the actual time, but rather some optimization steps. We want to choose an evolution law  $v$  such  $\frac{\partial J}{\partial t} < 0$ ,  $J$  will decrease with the artificial time evolution during a sufficient small time interval  $[0, \tau]$ .  $\frac{\partial J}{\partial t}$  is given by: (refer to Appendix A for the proof)

$$\frac{\partial J}{\partial t} = \int_S v \left[ \alpha \kappa + \frac{\partial \alpha}{\partial \vec{n}} \right] dS \quad (34)$$

where  $\vec{n}$  denotes the unit normal to the auxiliary surface  $S$  and

$$\alpha = \left[ \beta + \frac{1}{m} \sum_{p=1}^m \text{real} \left( \left\langle 2 \left( \int_S A(r') \vec{G}(|r' - r_p|) dS - \vec{f}(r_p) \right), A(r) \vec{G}(|r - r_p|) \right\rangle_{\mathbb{C}^3} \right) \right] \quad (35)$$

An obvious selection for  $v$  is

$$v = - \left( \alpha \kappa + \frac{\partial \alpha}{\partial \vec{n}} \right) \quad (36)$$

After substituting  $v$  into (33), differential equation can be solved numerically using the upwind scheme.

#### 4.2. Calculation of the Radiation Center Positions

Suppose  $\varphi$  is perturbed by a small variation  $\delta \varphi$  as shown in Figure 4. Let  $\delta r$  be the resulting variation of the point  $r$ .

By taking the variations of Equation (33) between  $t = 0$  and  $t = \tau$ , we get

$$\delta \varphi + v \tau \|\nabla \varphi\| = 0 \quad (37)$$

We have

$$v \tau = \delta r \quad (38)$$

We find the relation between  $\delta r$  and  $\delta\varphi$ .

$$\delta r = -\frac{\delta\varphi}{\|\nabla\varphi\|} \tag{39}$$

So, the radiations center positions  $r_{1 \leq i \leq n}$  are updated as follows.

$$r_i(t + \tau) = r_i(t) - \frac{\delta\varphi}{\|\nabla\varphi\|} \tag{40}$$

### 4.3. Calculation of the Auxiliary Sources' Amplitudes

To find the optimal auxiliary sources' amplitudes, we should update  $a_{1 \leq i \leq n}$  by following the descent direction of the cost function  $J$ . The descent direction is given by the negative derivative of  $J$  with respect to  $a_{1 \leq i \leq n}$ . So, we just need to compute  $\frac{\partial J}{\partial a_i}$  for  $1 \leq i \leq n$  and updating  $a_i$  as follows. Choose the step size  $\alpha > 0$

$$a_i(t + \tau) = a_i(t) - \alpha \frac{\partial J}{\partial a_i} \tag{41}$$

$\frac{\partial J}{\partial a_i}$  is given by: (refer to Appendix B for the proof)

$$\frac{\partial J}{\partial a_i} = \frac{1}{m} \sum_{p=1}^m \text{real} \left( \left\langle 2 \left( \sum_{k=1}^n a_k \vec{G}(|r_k - r_p|) - \vec{f}(r_p) \right), \vec{G}(|r_i - r_p|) \right\rangle_{\mathbb{C}^3} \right) \tag{42}$$

### 4.4. Numerical Scheme

To summarize we can list the optimization steps as below

- 1- Choose the initial level set function  $\varphi^0$  that represents the initial auxiliary surface  $S^0$ .
- 2- Choose the initial positions and amplitudes of the radiation centers  $(r_{1 \leq i \leq n}^0, a_{1 \leq i \leq n}^0)$ .
- 3- For  $j \geq 1$ 
  - Choose the regularization coefficient  $\beta$  and calculate  $v$

$$v = - \left( \alpha \kappa + \frac{\partial \alpha}{\partial \bar{n}} \right) \tag{43}$$

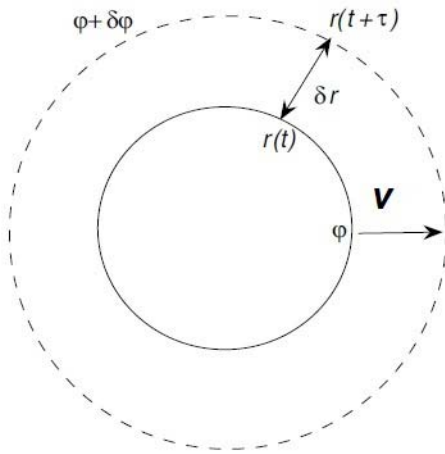


**Figure 4.** Deformation of shapes by the level set formulation.

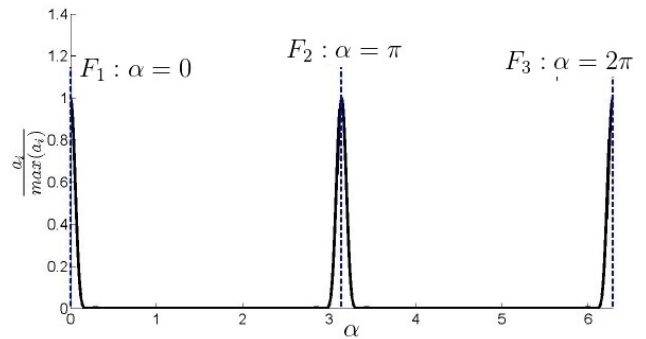


**Figure 5.** Singularities location of an elliptical cylinder.

- Determine the level set function  $\varphi^j$  by resolving the Hmilton-Jaccobi equation in the time interval  $[0, \tau]$  with the initial condition  $\varphi = \varphi^{j-1}$

$$\frac{\partial \varphi}{\partial t} + \|\nabla \varphi\| v = 0 \quad (44)$$

- update  $r_i^j$

$$r_i^j = r_i^{j-1} - \frac{\delta \varphi}{\|\nabla \varphi\|} \quad (45)$$

- Choose the step size  $\alpha^j$  and update  $a_i^j$

$$a_i^j = a_i^{j-1} - \alpha^j \frac{\partial J}{\partial a_i} \quad (46)$$

- Go to the next iteration if not converged.

The error of the boundary condition is used for convergence criterion

$$e_{p, 1 \leq p \leq m} = \frac{\left\| \int_S A(r') \vec{G}(|r' - x_p|) dS - \vec{f}(x_p) \right\|}{\left\| \vec{f}(x_p) \right\|} \quad (47)$$

Iterations continue until the stop criterion will be satisfied, typically when the errors  $e_{p, 1 \leq p \leq m}$  exhibit, between two iterations, become smaller than a predefined threshold. The proposed optimization procedure provides three degrees of freedom (auxiliary surface, positions and amplitudes of the radiation centers) to achieve any boundary condition error, which is a great advantage over classical MAS implementations. Indeed, in the classical MAS implementations, the auxiliary surface and the radiation center positions are fixed beforehand. So, the accuracy is not automatically adjustable, the only degree of freedom is the auxiliary sources' amplitudes. Generally, The standard MAS is based on empirical rules and on the caustic concept leading to the following recommendation [8]: The distance  $d$  between the physical surface  $\Gamma$  and the auxillary surface  $S$  should satisfy the condition  $d < R_{\min}$ , where  $R_{\min}$  is the minimal radius of positive curvature of the surface  $\Gamma$ . Several numerical methods have been proposed to overcome these constraints for the case of two-dimensional scattering problems, such as [9, 10]. By using Level set technique, the proposed method shows a great potential to determine the optimal MAS parameters that satisfy any accuracy.

## 5. NUMERICAL EXPERIMENTS

To complete this study we present two numerical examples. The aim of the first one is to show the ability of the proposed scheme to locate scattered field singularities. The second example is about radar cross section computing, we compare the accuracy and the computational cost obtained by the optimized MAS and those obtained by the standard MAS implementation. We consider perfectly conducting obstacles coated by a thin dielectric ( $\varepsilon = 2$ ) layer of thickness  $h = 0.1$ .

### 5.1. Singularities Localization of an Elliptical Cylinder

We consider an elliptical cylinder illuminated by an incident plane wave at 100 MHz. The scattered field has phase centers located in the ellipsoid foci's region [8]. The Figure 5 shows the auxiliary surface evolution at 0, 23, 50 and 70 iterations. The angle  $\alpha$  (Figures 5 and 6) is used to indicate the positions of the elementary sources on the auxiliary surface.

At the iteration 70, where the boundary condition error does not exceed 1%, the distribution of the sources' amplitudes for different angle  $\theta$  is shown in Figure 6. It is seen that for particular angles  $\alpha \in \{0, \pi, 2\pi\}$  the sharpest amplitude is observed. These angles correspond to the positions of foci  $F_1$  and  $F_2$ . The obtained surface passes through the foci's region, which is consistent with the analytic result.



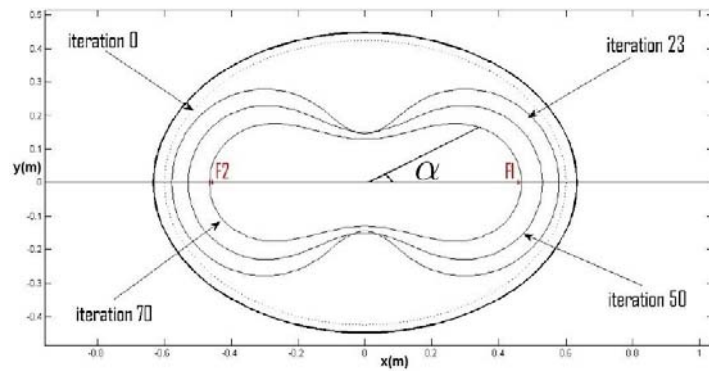


Figure 6. The distribution of the auxiliary sources amplitudes.

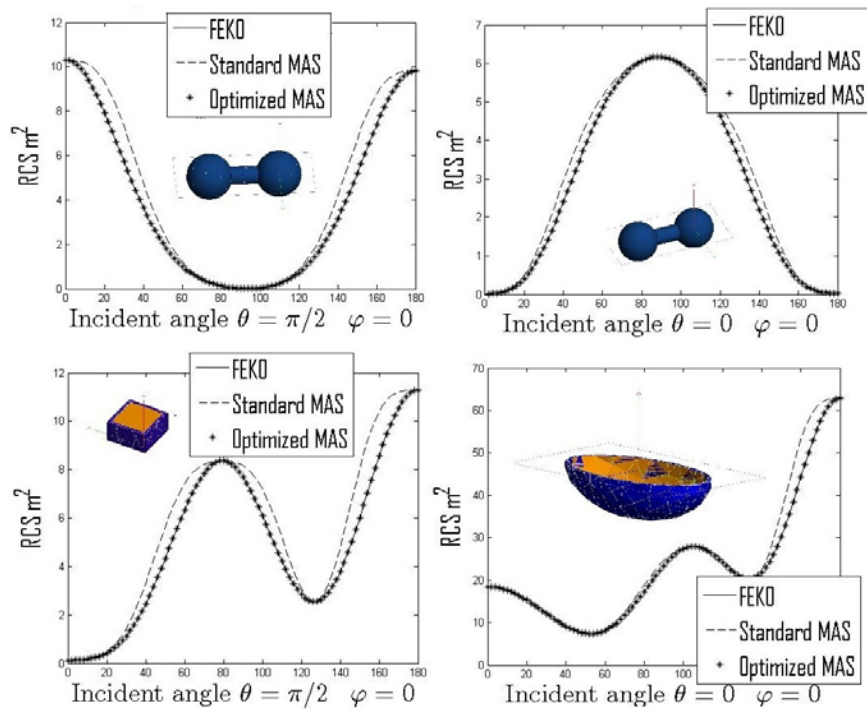


Figure 7. Comparison between the bistatic RCS values obtained from the optimized MAS and those obtained by the standard MAS implementation.

### 5.2. Accuracy and Computational Cost Evaluation

We present numerical experiments for some canonical geometries: coated dumbbell, coated ellipsoid and coated smoothed cuboid. All these obstacles are illuminated by an incident plane wave at  $f = 100$  MHz. Figure 7 shows a comparison between the bistatic RCS values obtained from the optimized MAS and those obtained by the standard implementation, the result from FEKO electromagnetic simulation software is taken as reference. Tables 1 and 2 show comparison between the optimized and the standard MAS method, the following criteria are taken into account: achieved accuracy (error on the boundary condition), number of auxiliary sources and number of collocation points.

As a conclusion of these numerical experiments, it appears clearly that the optimized method is able to achieve high accuracy with less implementation cost than the standard MAS implementation.

**Table 1.** Results obtained by the standard MAS implementation.

	Standard MAS		
	Accuracy	Auxiliary sources	Collocation points
<i>Coated smoothed cuboid</i>	5%	300	300
<i>Coated dumbbell</i>	7%	400	400
Coated ellipsoid	5%	300	300

**Table 2.** Results obtained by the optimized MAS.

	Optimized MAS		
	Accuracy	Auxiliary sources	Collocation points
<i>Coated smoothed cuboid</i>	0.1%	50	300
<i>Coated dumbbell</i>	0.2%	90	400
Coated ellipsoid	0.1%	60	300

## 6. CONCLUSION

We have reported a numerical framework for determining the optimal MAS parameters for three-dimensional scattering problems by combining the level set technique and the Generalized Impedance Boundary Conditions. The comparison between the radar cross section values obtained from the proposed framework and those obtained from the standard MAS implementation shows that the proposed method can achieve high accuracy with less implementation cost.

## APPENDIX A.

Let  $V$  the real Hilbert space of measurable functions over  $\Omega$ . the inner product  $\langle \cdot, \cdot \rangle$  is defined by

$$\forall (\phi, \psi) \in V^2 \quad \langle \phi, \psi \rangle_v = \int_{\Omega} \phi \psi d\Omega \quad (\text{A1})$$

We define the functions  $f$ ,  $g$  and  $F$  as follows

$$f : V \mapsto \mathbb{R}$$

$$X \rightarrow \left\| \int_{\Omega} \vec{u}(r') X(r') d\Omega - \vec{a} \right\|_{\mathbb{C}^3}^2 + \beta \int_{\Omega} X(r') d\Omega \quad (\text{A2})$$

$$g : V \mapsto V$$

$$\varphi \rightarrow \|\nabla \varphi\|_{\mathbb{C}^3} \delta(\varphi) \quad (\text{A3})$$

$F$  is the composition of functions  $f$  and  $g$

$$F : V \mapsto \mathbb{R}$$

$$\varphi \rightarrow f \circ g(\varphi) \quad (\text{A4})$$

where  $\vec{u}(r')$  is a vector field of  $\mathbb{C}^3$ ,  $\vec{a}$  a constant vector,  $\beta$  a positive coefficient, and  $\|\cdot\|_{\mathbb{C}^3}$  the usual norm of  $\mathbb{C}^3$ . By applying the chain's rule, we get

$$\frac{\partial F}{\partial \varphi} = \frac{\partial f}{\partial X}(g) \circ \frac{\partial g}{\partial \varphi} \quad (\text{A5})$$

By applying the definition of the Gateaux differential we get

$$\begin{aligned} & \frac{\partial f}{\partial X} : V \mapsto \mathbb{R} \\ & h \rightarrow \text{real} \left( \left\langle 2 \left( \int_{\Omega} \vec{u}(r') X(r') d\Omega - \vec{a} \right), \int_{\Omega} \vec{u}(r'') h d\Omega \right\rangle_{\mathbb{C}^3} \right) + \beta \int_{\Omega} h d\Omega \end{aligned} \quad (\text{A6})$$

and

$$\begin{aligned} \frac{\partial g}{\partial \varphi} : V &\mapsto V \\ h &\rightarrow \|\nabla\varphi\| \delta'(\varphi) + \delta(\varphi) \left\langle \frac{\nabla\varphi}{\|\nabla\varphi\|}, \nabla h \right\rangle \end{aligned} \tag{A7}$$

$\frac{\partial f}{\partial X}$  can be written in the following form

$$\begin{aligned} \frac{\partial f}{\partial X} : V &\mapsto \mathbb{R} \\ h &\rightarrow \int_{\Omega} \alpha(X) h d\Omega \end{aligned} \tag{A8}$$

where

$$\alpha(X) = \left[ \beta + \text{real} \left( \left\langle 2 \left( \int_{\Omega} \vec{u}(r') X(r') d\Omega - \vec{a} \right), \vec{u}(r'') \right\rangle_{\mathbb{C}^3} \right) \right] \tag{A9}$$

So,

$$\begin{aligned} \frac{\partial F}{\partial \varphi} : V &\mapsto \mathbb{R} \\ h &\rightarrow \int_{\Omega} \alpha(X) \left[ \|\nabla\varphi\| \delta'(\varphi) + \delta(\varphi) \left\langle \frac{\nabla\varphi}{\|\nabla\varphi\|}, \nabla h \right\rangle \right] d\Omega \end{aligned} \tag{A10}$$

We deduce

$$\frac{\partial F}{\partial t} = \frac{\partial F}{\partial \varphi} \circ \frac{\partial \varphi}{\partial t} = \int_{\Omega} \alpha \left[ \|\nabla\varphi\| \delta'(\varphi) \frac{\partial \varphi}{\partial t} + \delta(\varphi) \left\langle \frac{\nabla\varphi}{\|\nabla\varphi\|}, \nabla \left( \frac{\partial \varphi}{\partial t} \right) \right\rangle \right] d\Omega \tag{A11}$$

where

$$\alpha = \left[ \beta + \text{real} \left( \left\langle 2 \left( \int_S \vec{u}(r') dS - \vec{a} \right), \vec{u}(r'') \right\rangle_{\mathbb{C}^3} \right) \right] \tag{A12}$$

By using (35)

$$\frac{\partial F}{\partial t} = - \int_{\Omega} \alpha \left[ \|\nabla\varphi\| \|\nabla\varphi\| v \delta'(\varphi) + \delta(\varphi) \left\langle \frac{\nabla\varphi}{\|\nabla\varphi\|}, \nabla(v \|\nabla\varphi\|) \right\rangle \right] d\Omega \tag{A13}$$

We have

$$\left\langle \frac{\nabla\varphi}{\|\nabla\varphi\|}, \nabla(v \|\nabla\varphi\|) \right\rangle = \left\langle \frac{\nabla\varphi}{\|\nabla\varphi\|}, \|\nabla\varphi\| \nabla v + v \nabla(\|\nabla\varphi\|) \right\rangle \tag{A14}$$

The evolution of  $\varphi$  verify the constant normal extension

$$\left\langle \frac{\nabla\varphi}{\|\nabla\varphi\|}, \nabla v \right\rangle = \langle \vec{n}, \nabla v \rangle = 0 \tag{A15}$$

Also we have  $\delta'(\varphi) \nabla\varphi = \nabla(\delta(\varphi))$ . So,

$$\frac{\partial F}{\partial t} = - \int_{\Omega} \alpha \left[ \langle \nabla(\delta(\varphi)), v \nabla\varphi \rangle + \delta(\varphi) \left\langle \frac{\nabla\varphi}{\|\nabla\varphi\|}, v \nabla(\|\nabla\varphi\|) \right\rangle \right] d\Omega \tag{A16}$$

By using Gauss-Theorem

$$\frac{\partial F}{\partial t} = \int_{\Omega} \delta(\varphi) \left[ \text{div} \left( \alpha v \|\nabla\varphi\| \frac{\nabla\varphi}{\|\nabla\varphi\|} \right) - \alpha v \left\langle \frac{\nabla\varphi}{\|\nabla\varphi\|}, \nabla(\|\nabla\varphi\|) \right\rangle \right] d\Omega \tag{A17}$$

So,

$$\frac{\partial F}{\partial t} = \int_{\Omega} \delta(\varphi) \|\nabla\varphi\| v \left[ \alpha \text{div} \left( \frac{\nabla\varphi}{\|\nabla\varphi\|} \right) + \left\langle \frac{\nabla\varphi}{\|\nabla\varphi\|}, \nabla\alpha \right\rangle \right] d\Omega \tag{A18}$$

Finally, we get

$$\frac{\partial F}{\partial t} = \int_S v \left[ \alpha \kappa + \frac{\partial \alpha}{\partial \vec{n}} \right] dS \tag{A19}$$

## APPENDIX B.

Let  $V$  the real Hilbert space of measurable functions over  $\Omega$ . the inner product  $\langle \cdot, \cdot \rangle$  is defined by

$$\forall (\phi, \psi) \in V^2 \quad \langle \phi, \psi \rangle_v = \int_{\Omega} \phi \psi d\Omega \quad (\text{B1})$$

We define the functions  $f$ ,  $g$  and  $F$  as follows

$$f : V \mapsto \mathbb{R}$$

$$X \rightarrow \left\| \int_{\Omega} \vec{u}(r') X(r') d\Omega - \vec{a} \right\|_{\mathbb{C}^3}^2 \quad (\text{B2})$$

$$g : V \mapsto V$$

$$\varphi \rightarrow \theta \delta(r - r_0) \quad (\text{B3})$$

$F$  is the composition of functions  $f$  and  $g$

$$F : V \mapsto \mathbb{R}$$

$$\varphi \rightarrow f \circ g(\varphi) \quad (\text{B4})$$

where  $\vec{u}(r')$  a vector field of  $\mathbb{C}^3$ ,  $\vec{a}$  a constant vector,  $(\theta, r_0) \in \mathbb{R}^2$  and  $\|\cdot\|_{\mathbb{C}^3}$  the usual norm of  $\mathbb{C}^3$ . By applying the chain's rule, we get  $\frac{\partial F}{\partial \theta} = \frac{\partial f}{\partial X}(g) \circ \frac{\partial g}{\partial \theta}$ . By applying the definition of the Gateaux differential we get

$$\begin{aligned} \frac{\partial f}{\partial X} : V \mapsto \mathbb{R} \\ h \rightarrow \text{real} \left( \left\langle 2 \left( \int_{\Omega} \vec{u}(r') X(r') d\Omega - \vec{a} \right), \int_{\Omega} \vec{u}(r'') h d\Omega \right\rangle_{\mathbb{C}^3} \right) \end{aligned} \quad (\text{B5})$$

$$\begin{aligned} \frac{\partial g}{\partial \theta} : V \mapsto V \\ h \rightarrow \delta(r - r_0) \end{aligned} \quad (\text{B6})$$

So,

$$\begin{aligned} \frac{\partial F}{\partial \theta} : V \mapsto \mathbb{R} \\ h \rightarrow \text{real} (\langle 2(\theta \vec{u}(r_0) - \vec{a}), \vec{u}(r_0) \rangle_{\mathbb{C}^3}) \end{aligned} \quad (\text{B7})$$

## REFERENCES

1. Popovidi-Zaridze, R., D. Karkashadze, G. Ahvlediani, and J. Khatiashvili, "Investigation of possibilities of the method of auxiliary sources in solution of two-dimensional electrodynamic problems," *Radiotech. Electron.*, Vol. 22, No. 2, 1978.
2. Aleksidze, M. A., *Solution of Boundary Problems by Expansion into a Nonorthogonal Series*, Nauka, Moscow, 1978.
3. Aleksidze, M. A., *Fundamental Functions in Approximate Solutions of the Boundary Problems*, Nauka, Moscow, 1991.
4. Kupradze, V. D. and M. A. Aleksidze, "On one approximate method for solving boundary problems," *The BULLETIN of the Georgian Academy of Sciences*, 529–536, 1963.
5. Kupradze, V., "About approximates solution mathematical physics problem," *Success Math. Sci.*, Vol. 22, No. N2, 59107, 1967.
6. Popovidi-Zaridze, R. S. and Z. S. Tsverikmazashvili, "Numerical study of a diffraction problems by a modified method of nonorthogonal series," (in Russian, English translation available, translated and reprinted by Scientific Translation Editor, Oxford, 1978), *Zurnal. Vichislit. Mat. Mat Fiz.*, Vol. 17, No. 2, 1977.

7. Karkashadze, D. and R. Zaridze, "The method of auxiliary sources in applied electrodynamics," *LATSIS Symp.*, Zurich, 1995.
8. Bouzidi, A. and T. Aguilí, "Numerical optimization of the method of auxiliary sources by using level set technique," *Progress In Electromagnetics Research B*, Vol. 33, 203–219, 2011.
9. Tsitsasa, N. L., E. G. Alivizatosa, H. T. Anastassiua, and D. I. Kaklamania, "Optimization of the method of auxiliary sources (MAS) for scattering by an infinite cylinder under oblique incidence," *Electromagnetics*, Vol. 25, No. 1, 2006.
10. Anastassiu, H. T. and D. I. Kaklamani, "Error estimation and optimization of the method of auxiliary sources (MAS) applied to TE scattering by a perfectly conducting circular cylinder," *Journal of Electromagnetic Waves and Applications*, Vol. 18, No. 10, 1283–1294, 2004.
11. Okuno, Y., "A duality relationship between scattering field and current density calculation in the yasuura method," *MMET*, 278–281, 1994.
12. Zaridze, R., G. Bit-Babik, K. Tavzarashvili, N. Uzunoglu, and D. Economou, "Wave field singularity aspects large-size scatterers and inverse problems," *IEEE Transactions on AP*, Vol. 50, No. 1, 50–58, Jan. 2002.
13. Yuferev, S. V. and N. Ida, "Selection of the surface impedance boundary conditions for a given problem," *IEEE Trans. Magn.*, Vol. 35, No. 3, 1486–1489, 1999.
14. Antoine, X., H. Barucq, and L. Vernhet, "High-frequency asymptotic analysis of a dissipative transmission problem resulting in generalized impedance boundary conditions," *Asymptot. Anal.*, Vol. 26, No. 3–4, 257–283, 2001.
15. Kupradze, V., *Method of Integral Equations in the Theory of Diffraction*, Moscow-Leningrad, 1935.
16. Osher, S. and J. A. Sethian, "Fronts propagating with curvature-dependent speed: Algorithms based on Hamilton-Jacobi formulations," *Journal of Computational Physics*, Vol. 79, 1249, 1988.
17. Osher, S. and R. P. Fedkiw, "Level set methods: An overview and some recent results," *J. Comput. Phys.*, 463–502, 2001.
18. Sethian, J. A., "Level set methods and fast marching methods," Volume 3 of *Cambridge Monographs on Applied and Computational Mathematics*, 2nd Edition, Cambridge University Press, Cambridge, 1999. Evolving interfaces in computational geometry, fluid mechanics, computer vision, and materials science.
19. Tai, X.-C. and T. F. Chan, "A survey on multiple level set methods with applications for identifying piecewise constant functions," *International J. Numerical Analysis and Modelling*, Vol. 1, No. 1, 25–48, 2004.
20. Anastassiu, H., "Error estimation of the method of auxiliary sources (MAS) for scattering from an impedance circular cylinder," *Progress In Electromagnetics Research*, Vol. 52, 109–128, 2005.
21. Hichem, N. and T. Aguilí, "Scattering by multilayered structures using the extended method of auxiliary sources EMAS," *Progress In Electromagnetics Research B*, Vol. 15, 133–150, 2009.
22. Hichem, N. and T. Aguilí, "Analysis of two-dimensional scattering by a periodic array of conducting cylinders using the method of auxiliary sources," *PIERS Online*, Vol. 4, No. 5, 521–525, 2008.
23. Hichem, N. and T. Aguilí, "Analysis of scattering from a finite linear array of dielectric cylinders using the method of auxiliary sources," *PIERS Proceedings*, 743–746, Beijing, China, Mar. 23–27, 2009.
24. Hichem, N. and T. Aguilí, "Modeling the electromagnetic scattering from a dielectrically filled groove using the method of auxiliary sources," *PIERS Proceedings*, 858–860, Beijing, China, Mar. 23–27, 2009.
25. Bogdanov, F. G., D. D. Karkashadze, and R. S. Zaridze, "The method of auxiliary sources in electromagnetic scattering problems," *Generalized Multipole Techniques for Electromagnetic and Light Scattering*, 1999.
26. Wriedt, T., *Generalized Multipole Techniques for Electromagnetic and Light Scattering*, Elsevier, Amsterdam, New York, 1999.